four transitions turn out to be optically active, whereas in (001) quantum dots the parameter g_{h2} is zero, implying that $C_2 \equiv 0$ and that only two recombination processes are allowed. It should be emphasized that the mixing effect of $\pm 3/2$ states in a longitudinal magnetic field can show its worth in trigonal systems with arbitrary dimensionality $d = 0-3$, including an exciton in Ge crystals formed by an L-valley electron and a Γ_8^+ hole and bound on a neutral donor [38].

A nonzero value g_{h2} of the g factor can be obtained by noting that in bulk zinc blende lattice semiconductors the Zeeman interaction of Γ_8 holes with a magnetic field is described by the Hamiltonian

$$\mathcal{H}_{\mathbf{B}}^{(\Gamma_8)} = -2\mu_{\mathrm{B}}\left[\kappa \mathbf{J}\,\mathbf{B} + q(J_x^3 B_x + J_y^3 B_y + J_z^3 B_z)\right], \quad (13)$$

which contains two dimensionless coefficients, κ and q. Here, x, y and z are the crystallographic axes [100], [010] and [001], and J_x, J_y, and J_z are the angle momentum matrices in the Γ_8 basis. Let us go over in Hamiltonian (13) to the coordinates $x' \| [11\bar{2}]$, $y' \| [\bar{1}10]$, $z' \| [111]$ and introduce the basis functions $|3/2\rangle'$, $|-3/2\rangle'$, which transform according to the reducible representation $\mathcal{D} = \Gamma_5 + \Gamma_6$ of the C_{3v} group. Then, the Zeeman splitting in the field $\mathbf{B} \| [111]$ will be described by a 2×2 matrix with $g_{h1} = -6\kappa$, and $g_{h2} = 2\sqrt{2}q$.

Acknowledgments. This work was supported by an RAS Presidium Program and by RFBR grants. The author is grateful to M M Glasov for helpful discussions of the manuscript.

References

1. Dyakonov M I (Ed.) *Spin Physics in Semiconductors* (Berlin: Springer, 2008)
2. Kusrayev Yu, Landwehr G (Guest Eds) *Semicond. Sci. Technol.* **23** (11) (2008), Special issue on optical orientation
3. *Fiz. Tekh. Poluprovodn.* **42** (8) (2008) [*Semicond.* **42** (8) (2008)], Vladimir Idelevich Perel' (on the 80th anniversary of his birthday), Special issue
4. Ivchenko E L, Kiselev A A *Fiz. Tekh. Poluprovodn.* **26** 1471 (1992) [*Sov. Phys. Semicond.* **26** 827 (1992)]
5. Kiselev A A, Ivchenko E L, Rössler U *Phys. Rev. B* **58** 16353 (1998)
6. Yugova I A et al. *Phys. Rev. B* **75** 245302 (2007)
7. Durnev M V, Glazov M M, Ivchenko E L *Physica E* **44** 797 (2012); arXiv:1111.6837
8. Rashba E I *Fiz. Tverd. Tela* **2** 1224 (1960) [*Sov. Phys. Solid State* **2** 1109 (1960)]
9. Bychkov Yu A, Rashba E I *Pis'ma Zh. Eksp. Teor. Fiz.* **39** 66 (1984) [*JETP Lett.* **39** 78 (1984)]
10. Ivchenko E L *Optical Spectroscopy of Semiconductor Nanostructures* (Harrow, UK: Alpha Sci. Intern. Ltd, 2005)
11. Nestoklon M O, Golub L E, Ivchenko E L *Phys. Rev. B* **73** 235334 (2006)
12. Glazov M M, Ivchenko E L *Pis'ma Zh. Eksp. Teor. Fiz.* **75** 476 (2002) [*JETP Lett.* **75** 403 (2002)]
13. Glazov M M, Ivchenko E L *Zh. Eksp. Teor. Fiz.* **126** 1465 (2004) [*JETP* **99** 1279 (2004)]
14. Leyland W J H et al. *Phys. Rev. B* **75** 165309 (2007)
15. Ivchenko E L, Pikus G E *Superlattices and other Heterostructures: Symmetry and Optical Phenomena* (Berlin: Springer-Verlag, 1995); *Superlattices and other Heterostructures: Symmetry and Optical Phenomena* 2nd ed. (Berlin: Springer, 1997)
16. Ivchenko E L *Phys. Status Solidi A* **164** 487 (1997)
17. Gupalov S V, Ivchenko E L, Kavokin A V *Zh. Eksp. Teor. Fiz.* **113** 703 (1998) [*JETP* **86** 388 (1998)]
18. Sallen G et al. *Phys. Rev. Lett.* **107** 166604 (2011)
19. Stevenson R M et al. *Phys. Rev. B* **73** 033306 (2006)
20. Glazov M M et al. *Phys. Rev. B* **76** 193313 (2007)
21. Kusrayev Yu G *Usp. Fiz. Nauk* **180** 759 (2010) [*Phys. Usp.* **53** 725 (2010)]
22. Glazov M M, Yugova I A, Efros Al L *Phys. Rev. B* **85** 041303(R) (2012); arXiv:1103.3249
23. Glazov M M *Fiz. Tverd. Tela* **54** 3 (2012) [*Phys. Solid State* **54** 1 (2012)]
24. Ivchenko E L *Fiz. Tekh. Poluprovodn.* **7** 1489 (1973) [*Sov. Phys. Semicond.* **7** 998 (1973)]
25. Müller G M et al. *Physica E* **43** 569 (2010)
26. Aleksandrov E B, Zapasskii V S *Zh. Eksp. Teor. Fiz.* **81** 132 (1981) [*Sov. Phys. JETP* **54** 64 (1981)]
27. Crooker S A et al. *Phys. Rev. Lett.* **104** 036601 (2010)
28. Glazov M M, Sherman E Ya *Phys. Rev. Lett.* **107** 156602 (2011)
29. Ivchenko E L, Pikus G E *Pis'ma Zh. Eksp. Teor. Fiz.* **27** 640 (1978) [*JETP Lett.* **27** 604 (1978)]
30. Ivchenko E L *Usp. Fiz. Nauk* **172** 1461 (2002) [*Phys. Usp.* **45** 1299 (2002)]
31. Ivchenko E L, Ganichev S D, in *Spin Physics in Semiconductors* (Ed. M I Dyakonov) (Berlin: Springer, 2008) p. 245
32. Aronov A G, Ivchenko E L *Fiz. Tverd. Tela* **15** 231 (1973) [*Sov. Phys. Solid State* **15** 160 (1973)]
33. Glazov M M et al. *Phys. Rev. B* **82** 155325 (2010)
34. Greilich A et al. *Science* **313** 341 (2006)
35. Yugova I A et al. *Phys. Rev. B* **80** 104436 (2009)
36. Haken H *Light* Vol. 2 *Laser Light Dynamics* (Amsterdam: North-Holland, 1985) [Translated into Russian (Moscow: Mir, 1988)]
37. Dzhioev R I et al. *Pis'ma Zh. Eksp. Teor. Fiz.* **65** 766 (1997) [*JETP Lett.* **65** 804 (1997)]
38. Averkiev N S et al. *Fiz. Tverd. Tela* **23** 3117 (1981) [*Sov. Phys. Solid State* **23** 1815 (1981)]

PACS numbers: 72.25.Hg, 72.25.Pn, 72.25.Rb, 73.63.Hs
DOI: 10.3367/UFNe.0182.201208h.0876

Spin transport in heterostructures

L E Golub

1. Introduction. Spin splittings

In the absence of an external magnetic field, electronic states can be spin-split if the system has no space inversion center. The reason for these spin splittings is the spin–orbit interaction. The simplest example of a noncentrosymmetric medium is a surface. The Hamiltonian of the spin-orbit interaction in a half-infinite medium assumes the following (Rashba [1, 2]) form:

$$H_{\mathrm{so}} = \alpha(\boldsymbol{\sigma} \times \mathbf{k})\,\mathbf{n}\,. \quad (1)$$

Here, the vector $\boldsymbol{\sigma}$ is composed of Pauli matrices, $\mathbf{k}$ is the electron wave vector, α is a certain number, and $\mathbf{n}$ is a unit normal vector to the surface. This form of such spin–orbit interaction occurs in various noncentrosymmetric semiconductors, metals, and superconductors.

L E Golub Ioffe Physical Technical Institute,
Russian Academy of Sciences, St. Petersburg, Russian Federation
E-mail:golub@coherent.ioffe.ru

Uspekhi Fizicheskikh Nauk **182** (8) 876 – 879 (2012)
DOI: 10.3367/UFNr.0182.201208h.0876
Translated by E G Strel'chenko; edited by A Radzig

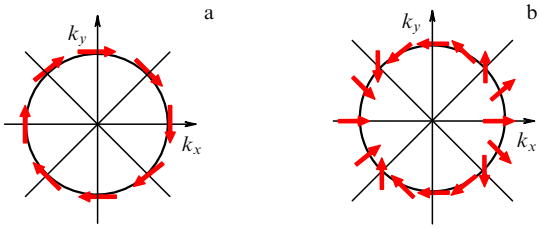

Figure 1. Effective magnetic field $\mathbf{\Omega}(\mathbf{k})$ for electrons (a) and polaritons (b).

In addition to expression (1), an interaction of a different form — Dresselhaus — occurs in heterostructures grown from noncentrosymmetric semiconductors (for example, GaAs). The Hamiltonian of any type of such interaction has the form $H_{so} \propto \sigma_i k_j$, $\sigma_i k_j k_l k_m$ and can be conveniently written down in the Zeeman form

$$H_{so} = \frac{\hbar}{2}\,\boldsymbol{\sigma}\,\mathbf{\Omega}(\mathbf{k})\,. \qquad (2)$$

Here, the effective Larmor frequency $\mathbf{\Omega}(\mathbf{k})$ is a pseudovector odd in $\mathbf{k}$. The spin splitting energy is $\Delta_{so}(\mathbf{k}) = \hbar|\mathbf{\Omega}(\mathbf{k})|$. The directions of $\mathbf{\Omega}(\mathbf{k})$ in $\mathbf{k}$ space for the Rashba interaction are shown by arrows in Fig. 1a. In real heterostructures, both types of splitting exist. Their interference results in suppressing electron spin relaxation for one of the spin orientations in the plane of a structure grown along the [001] direction if the Rashba and Dresselhaus fields are equal in magnitude [3–5]. Based on these ideas, a model of a spin transistor capable of realizing diffusive spin transport was proposed [6].

2. Weak localization of electrons and exciton polaritons

A transport phenomenon which clearly displays spin splittings is weak localization — an effect consisting in enhanced backward scattering due to the interference of the incident and scattered waves. There are a variety of pathways for a wave propagating through a system of scatterers, some of them forming a special class of self-intersecting or loop-containing trajectories. Trajectories with loops following clockwise and counterclockwise are accounted for independently, and the phase incursions of the wave passing along these trajectories are equal. As a result, the waves reflected after passing along two such trajectories interfere, and the passage through a system of scatterers becomes less probable than in a classical calculation. Such a reduction in passage is a localization in character, even though it occurs for freely propagating particles, which is the reason why this phenomenon — enhanced backward scattering — came to be known as the *weak localization* effect.

Because of their wave properties, electrons also exhibit this effect, if to a small degree. In electronic systems, weak localization shows its worth as a decrease in conductivity, as opposed to the classical Drude value σ_{cl}. The correction to the conductivity due to the weak localization is equal to $\Delta\sigma_{WL} \sim (\lambda/l)\,\sigma_{cl}$, where λ is the de Broglie wavelength, and l is the electron mean free path. As a result, we have $\Delta\sigma_{WL} \sim e^2/\hbar$ [7].

What is remarkable about the correction $\Delta\sigma_{WL}$ is its sensitivity to a classically weak magnetic field which does not produce a considerable Lorentz force. The field dependence is due to the fact that electron waves that have passed a self-intersecting trajectory in two opposite directions differ in phase by an amount equal to the magnetic field flux through the loop. As a result, the field destroys the wave interference, and the conductivity returns to its classical value, i.e. increases. There are a variety of semiconductors, metals, and heterostructures that exhibit positive magnetoconductivity or negative magnetoresistance. This magnetoresistance is referred to as *anomalous* due to its strong dependence on the magnetic field and temperature.

The presence of spin splittings we touched upon in the Introduction changes the weak localization picture markedly. From Fig. 1a it is seen that, if the spin follows the change in the effective field $\mathbf{\Omega}$, a clockwise or counterclockwise path tracing imparts to the electron a (Berry) phase equal to $\pm\pi$. Considering the existence of an electron spin, this difference in sign is significant, because the wave function of a backward scattered electron differs by a factor $\pm$i from the incident wave function. As a result, the constructive interference becomes destructive, the backward scattering is suppressed rather than enhanced, the correction to the conductivity is positive, and the magnetic field destroying this correction leads to positive magnetoresistance. Because all this is opposite to the spinless case, this mode of electron behavior is called *weak antilocalization*. In the case of moderately strong spin–orbit interaction, when Δ_{so} is much less than the Fermi energy, the time between collisions is too short for an electron to fully align along the field $\mathbf{\Omega}$, so that magnetoresistance is sign-variable and is represented by a curve with a maximum.

The mid-1990s theory [8] of weak localization for heterostructures with Rashba and Dresselhaus (see Eqn (2)) spin splittings was successful in describing magnetoresistance in low-mobility heterostructures available at the time [9]. Anomalous magnetoresistance was typically observed in much weaker magnetic fields than the 'transport' field in which the magnetic length becomes equal to the electron mean free path, $B_{tr} = \hbar/(2el^2)$.

However, starting from the 2000s, experimental studies began to appear that demonstrated anomalous magnetoresistance in fields $B \lesssim B_{tr}$. The application of the theory developed in Ref. [8] sometimes led to meaningless fitting parameters. Especially challenging for theorists was the finding [10] that the formulas of Ref. [8] produce different fitting parameters for the decreasing and increasing portions of the magetoconductivity curve. It became clear that high-mobility heterostructures require for their description a new expression for anomalous magnetoresistance, which is suitable for both the diffusion and ballistic modes of weak antilocalization.

It was Ref. [11] which came up with the new theory. In the presence of the spin–orbit interaction (2), an electron which resided in one of the spin states $|\alpha\rangle$ before tracing the loop is, generally, in a different state, $|\beta\rangle$, after tracing it due to the spin having rotated in the effective field $\mathbf{\Omega}$. In accordance with the electron spin having two possible projections onto the growth axis before and after the loop tracing ($\alpha, \beta = \pm 1/2$), there are four interferential contributions to the conductivity. It is convenient to introduce two variables, the total electron moment $\mathbf{S}$ before and after tracing the loops, and its projection m onto the heterostructure growth axis. It turns out that the interference is constructive or destructive if, respectively, the electron spin states form a singlet ($S = 0$, $m = 0$) or a triplet ($S = 1$, $m = 0, \pm 1$) before and after the loop tracing. The correction to the conductivity is calculated

by the Green function method. In a magnetic field, the probability of backward scattering is calculated as a function of Landau level indices N. Whereas in the singlet channel all Landau levels contribute independently, in the triplet channel contributions from different levels are engaged. For example, independent contributions in the case of the Rashba interaction come from the states (N, m) with equal $N + m$: $(N, 1)$, $(N + 1, 0)$, and $(N + 2, -1)$, whereas in the case of the Dresselhaus interaction they come from those with equal $N - m$. In either case, the triplet contribution to the conductivity is described by the trace of a third-rank matrix [11]. According to the new theory, the magnetoconductivity may have its minimum equally well in fields larger and smaller than $B_{\rm tr}$. For $B \gg B_{\rm tr}$, the magnetoconductivity comes to the asymptotic value

$$\Delta\sigma_{\rm WL} = -0.25\sqrt{\frac{B_{\rm tr}}{B}}\,\frac{e^2}{\hbar}\,,$$

whatever the magnitude of the spin–orbit interaction.

The theory proved successful in describing experimental data on anomalous magnetoresistance in various heterostructures [12, 13]. Experimental results described by the theory for various temperatures and various concentrations of two-dimensional electrons are reviewed in Ref. [14].

Reference [15] considers anisotropic spin splitting for the case with both the Rashba and Dresselhaus contributions present. In this case, the contributions to $\Delta\sigma_{\rm WL}$ from different Landau levels do not break up in groups, and the triplet contribution is described by an infinite-rank matrix. In the case of a spin splitting cubic in the wave vector, which occurs for a high electron concentration, the triplet contribution is made by trios of states with equal values of $N + 3m$ [15]. The expressions obtained are also valid for hole type quantum wells, for which spin splitting is also cubic in the wave vector. The anomalous magnetoresistance in hole heterostructures has recently become a subject of study for several experimental groups simultaneously.

Weak localization comprises a wave interference phenomenon and, as such, also occurs for light. A suitable heterostructure system to study light interference is the microcavity. Experiments on the Rayleigh scattering of exciton polaritons demonstrate the enhancement of backward scattering [16]. In polarization-resolved measurements, light of different polarizations excites different polariton states. These are conveniently described by introducing the pseudospin vector $\mathbf{S}$ composed of the polarization Stokes parameters. The longitudinal–transverse splitting of polaritons is described by the same Hamiltonian (2) as the electron spin splitting, with the important difference that the effective Larmor frequency of polaritons is quadratic in their momenta in the microcavity plane, $\mathbf{k}$. Its directions in $\mathbf{k}$ space are shown in Fig. 1b. Due to the evenness of $\boldsymbol{\Omega}(\mathbf{k})$, the Berry phase — a phase incursion of a polariton as it traces a loop — equals 2π (if the spin follows the direction of $\boldsymbol{\Omega}$) rather than π, as for electrons. Therefore, polariton interference is constructive, backward scattering is enhanced, and localization takes place. As a result, backward scattering increases in intensity compared to scattering through other angles [17].

In polarization-resolved experiments, the scattering of polaritons with a fixed pseudospin projection can be studied separately. This makes a polariton system advantageously different from its electronic counterpart, in that in the latter the only quantity which is measured is the conductivity equal to a sum of the singlet and all the triplet interferential contributions. It turns out that for a pseudospin oriented in the microcavity plane (light is polarized linearly), the backward scattering intensity enhances, whereas for the pseudospin directed along the growth axis (circular polarization of light) it shows a dip [18]. If the cavity is nonsymmetric, the longitudinal–transverse splitting becomes anisotropic with respect to various directions of $\mathbf{k}$ in the plane of the structure, resulting in the difference in backscattering for two linear polarizations. Further still, interferential effects act to convert linear polarization to circular [18].

The presence of a longitudinal–transverse splitting also affects the classical dynamics of polarization in microcavities in which the multiple elastic light scattering mode is realized [19]. This requires that the polariton elastic scattering time τ_1 be much shorter than the lifetime τ_0. The kinetics of a polariton pseudospin is described by the equation [17]

$$\frac{\mathbf{S}_\mathbf{k}}{\tau_0} + \mathbf{S}_\mathbf{k} \times \boldsymbol{\Omega}(\mathbf{k}) + \frac{\mathbf{S}_\mathbf{k} - \langle \mathbf{S}_\mathbf{k} \rangle}{\tau_1} = \mathbf{g}_\mathbf{k}\,. \tag{3}$$

Here, $\mathbf{S}_\mathbf{k}$ is the pseudospin of a polariton with a wave vector $\mathbf{k}$, the angular brackets stand for averaging over the directions of $\mathbf{k}$, and $\mathbf{g}_\mathbf{k}$ is the generation rate to the $\mathbf{k}$ state. Pseudospin rotations in the field $\boldsymbol{\Omega}(\mathbf{k})$ lead to the emission of circularly polarized light when the exciting polarization is linear. Instead of the labor-consuming computer calculations that were done in Ref. [19], the kinetic theory of Ref. [18] can be used to describe the experimental results.

3. Spin orientation by electric current

The conversion of linearly polarized radiation to circularly polarized one is a special case of the more general transformation of translational motion to rotational. In electronic systems, an example of such a phenomenon is the electric current-assisted orientation of spin.

The appearance of spin $\mathbf{s}$ due to the flow of electric current with density $\mathbf{j}$ is described phenomenologically by the equality

$$s_i = Q_{im} j_m\,, \tag{4}$$

where $\hat{Q}$ is a second-rank pseudotensor. This relation applies only to gyrotropic media. Although bulk GaAs type semiconductors are not gyrotropic, the fact is that, virtually regardless of the material used to grow a heterostructure, its $\hat{Q}$ has nonzero components. Symmetry analysis shows that if gyrotropy is due to the structural asymmetry of the system (similar to the Rashba splitting), the spin aligns along the plane of the structure perpendicular to the current (Fig. 2a). The absence of a spatial inversion center in a bulk material (for example, in GaAs) leads, in addition to Dresselhaus

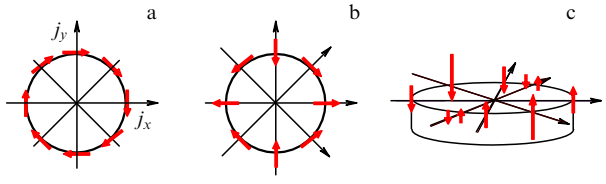

Figure 2. Spin orientation by current in (z-axis grown) heterostructures with strong structural asymmetry (a), and in A_3B_5 quantum dots with $z \parallel [001]$ (b) and $z \parallel [110]$ (c).

splitting, to the possibility of a spin being oriented by an electric current. In this case, the effect is crystallographically sensitive. In A_3B_5 heterostructures grown along the cubic [001]-axis, the current orients the spin to lie in the plane, as shown in Fig. 2b: parallel or perpendicular to the current depending, respectively, on whether the current flows along the axes [100], [010] or along [110], [1$\bar{1}$0]. In [110]-grown heterostructures, a current flowing along the [1$\bar{1}$0]-axis causes the spin to align along the growth axis (Fig. 2c).

Experimental studies of current-assisted spin orientation were carried out on heterostructures grown from GaAs, InAs, ZnSe, and GaN in different crystallographic directions [20–22].

The microscopic mechanism of spin orientation by current is related to the spin–orbit splitting (2). In an external electric field $\mathbf{E}$, the electronic system acquires a drift quasimomentum $\mathbf{k}_{dr} = e\mathbf{E}\tau_{tr}/\hbar$, where τ_{tr} is the mobility-controlling transport relaxation time. The presence of a finite quasimomentum formally implies a nonzero spin splitting $\mathbf{\Delta}_{so}(\mathbf{k}_{dr}) = \hbar\mathbf{\Omega}(\mathbf{k}_{dr})$ due to the effective magnetic field. As a result, spin polarization emerges, which, by analogy with the Zeeman effect, can be represented in the form

$$s = -c\,\frac{\mathbf{\Delta}_{so}(\mathbf{k}_{dr})}{\bar{E}}\,, \qquad (5)$$

where $\bar{E}$ is the average electron energy equal to the Fermi energy or the temperature in the degenerate and Boltzmann cases, respectively.

For a system in a real magnetic field, the constant c would be 1/4. For spin orientation by an electric field, this coefficient is also on the order of unity. However, a difference shows up in this case between the thermodynamic effect of spin orientation by a magnetic field and the kinetic effect of electric current-assisted spin orientation. In the presence of an electric field, the electron distribution in $\mathbf{k}$ space undergoes a shift in any of the spin branches and, taking into account the spin–orbit splittings of the energy spectrum, has the form shown in Fig. 3a. However, until there is no coupling between the spin subsystems, the spin up and spin down electrons are equal in number, thus preventing the appearance of an average spin. It is spin relaxation which allows the spin subbands to 'communicate'. The arrows in Fig. 3a indicate spin flip processes. It is seen that, if the probability of a spin flip scattering event depends on the momentum transfer, spin generation will occur: transitions from the spin-up subband to the spin-down subband and those in the opposite direction will occur at different rates. However, because spin relaxation is controlled by the same processes, the spin flip probability does not affect the stationary value of spin. This leaves us with formula (5) as the correct one — with the caveat, however, that theoretical studies (of which there are many) yield different values for c (for a review, see Ref. [23] and references cited therein). The spread is due to the fact that the degree of spin orientation depends on the ratio of the spin to energy relaxation rates. If energy relaxation processes are faster than those of spin relaxation, they rapidly mix spin between electrons of different energies. In this case, the spin distribution over energy is equilibrium, albeit $c = 1/2$, i.e. twice the value in a real magnetic field. In the opposite limit of slow energy relaxation, spin establishes itself for each energy independently. Although this results in $c = 1/4$, the distribution of spins over the energy is nonequilibrium [23]. Experimentally, energy relaxation processes are slow at temperatures from 4–10 K, but at higher temperatures energy relaxation becomes faster than the spin relaxation. For comparable values of energy and spin relaxation times, the coefficient c ranges between 1/4 and 1/2.

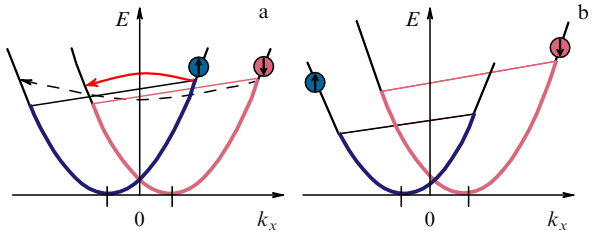

Figure 3. Microscopic picture of electric spin orientation. (a) Spin subband populations in the presence of an electric field. Spin–orbit splitting is taken into account, and spin relaxation processes are neglected. Solid and dashed arrows denote spin flip processes running with different probabilities. (b) Distribution in spin subbands due to spin relaxation processes.

Of interest is the case of symmetrically doped (110) quantum wells. In such systems, symmetry allows the normal spin component to be oriented by a current flowing along the [1$\bar{1}$0]-axis, but the Rashba spin splitting is zero, and the Dyakonov–Perel spin relaxation is absent. Allowing fluctuations in the position of a doping impurity makes a quantum well locally nonsymmetric, resulting in the fluctuation of the spin–orbit interaction and giving rise to spin relaxation [24]. This also enables current-assisted spin orientation but, remarkably, the coefficient c in formula (5) becomes a function of the correlation length of the spin–orbit field fluctuations [23]. Also of interest are the kinetics of current-assisted spin orientation in such a system, in particular, the fact of their becoming nonmonoexponential for slow energy relaxation [23].

Two-dimensional topological insulators realizable, for example, on the surface of three-dimensional Bi_2Se_3 compounds, are yet another class of systems allowing for spin orientation by current. The electronic spectrum of such systems is linear in the two-dimensional wave vector and is described by the effective Hamiltonian (1). Importantly, because of the absence of terms quadratic in k, contribution (1) is not a small correction in this case. Spin in topological insulators is oriented perpendicular to the current (see Fig. 2a), and its magnitude is $s = k_{dr}/(2k_F)$, with k_F being the Fermi wave vector [23]

Acknowledgments. This work was supported by RAS and RFBR programs, and by a grant from the President's Fund for Young Scientists.

References

1. Rashba E I *Fiz. Tverd. Tela* **2** 1224 (1960) [*Sov. Phys. Solid State* **2** 1109 (1960)]
2. Rashba E I *Usp. Fiz. Nauk* **84** 557 (1964) [*Sov. Phys. Usp.* **7** 823 (1965)]
3. Averkiev N S, Golub L E *Phys. Rev. B* **60** 15582 (1999)
4. Averkiev N S, Golub L E *Semicond. Sci. Technol.* **23** 114002 (2008)
5. Averkiev N S *Usp. Fiz. Nauk* **180** 777 (2010) [*Phys. Usp.* **53** 742 (2010)]
6. Schliemann J, Egues J C, Loss D *Phys. Rev. Lett.* **90** 146801 (2003)
7. Altshuler B L, Aronov A G, in *Electron-Electron Interactions in Disordered Systems* (Eds A L Efros, M Pollak) (Amsterdam: Elsevier, 1985) p. 1

8. Iordanskii S V, Lyanda-Geller Yu B, Pikus G E *Pis'ma Zh. Eksp. Teor. Fiz.* **60** 199 (1994) [*JETP Lett.* **60** 206 (1994)]
9. Knap W et al. *Phys. Rev. B* **53** 3912 (1996)
10. Studenikin S A et al. *Phys. Rev. B* **68** 035317 (2003)
11. Golub L E *Phys. Rev. B* **71** 235310 (2005)
12. Guzenko V A et al. *Phys. Status Solidi C* **3** 4227 (2006)
13. Yu G et al. *Phys. Rev. B* **78** 035304 (2008)
14. Glazov M M, Golub L E *Semicond. Sci. Technol.* **24** 064007 (2009)
15. Glazov M M, Golub L E *Fiz. Tekh. Poluprovodn.* **40** 1241 (2006) [*Semiconductors* **40** 1209 (2006)]
16. Gurioli M et al. *Phys. Rev. Lett.* **94** 183901 (2005)
17. Glazov M M, Golub L E *Phys. Rev. B* **77** 165341 (2008)
18. Glazov M M, Golub L E *Phys. Rev. B* **82** 085315 (2010)
19. Amo A et al. *Phys. Rev. B* **80** 165325 (2009)
20. Ganichev S D et al. *J. Magn. Magn. Mater.* **300** 127 (2006); cond-mat/0403641
21. Silov A Yu et al. *Appl. Phys. Lett.* **85** 5929 (2004)
22. Sih V et al. *Nature Phys.* **1** 31 (2005)
23. Golub L E, Ivchenko E L *Phys. Rev. B* **84** 115303 (2011)
24. Glazov M M, Sherman E Ya, Dugaev V K *Physica E* **42** 2157 (2010)

PACS numbers: 47.27.Gs, 47.35.Pq, 68.03.Kn
DOI: 10.3367/UFNe.0182.201208i.0879

Kinetic and discrete turbulence on the surface of quantum liquids

L V Abdurakhimov, M Yu Brazhnikov, A A Levchenko, I A Remizov, S V Filatov

1. Introduction

Wave turbulence is a nonequilibrium state in a system of interacting nonlinear waves in which the energy pumping and dissipation ranges are well separated in the wave number space. A turbulent state is characterized by a directed energy flux P in the k-space. Wave turbulence states can be realized in many nonlinear systems, for example, in plasmas [1], magnetic systems in solids [2], and on the surface of seas and oceans [3]. In our experiments, we explore the turbulence in a system of capillary waves, where surface tension plays the main role. Waves on a water surface are conventionally referred to as gravity waves if their wavelength exceeds 17 mm, and as capillary waves otherwise.

The frequency ω of capillary waves on the surface of a liquid is defined by the modulus of the wave vector k together with the surface tension coefficient σ and fluid density ρ:

$$\omega = \left(\frac{\sigma}{\rho}\right)^{1/2} k^{3/2} . \qquad (1)$$

Dispersion law (1) for capillary waves is of a decaying type, i.e., it permits the three-wave processes of wave decay into two waves or coalescence of two waves into a single wave while such that the energy and momentum are conserved,

$$\omega_1 \pm \omega_2 = \omega_3 , \qquad k_1 \pm k_2 = k_3 . \qquad (2)$$

When the surface of a liquid is excited by an external force, a turbulent state can develop in the system of capillary waves, in which the energy flux P in the k-space is directed from the pumping range toward large wave numbers (high frequencies), forming a direct cascade. Under the assumption that wave interactions are weak and hence the main contribution to energy transfer comes from three-wave processes, the theory of (weak) wave turbulence [4] predicts a power law for the energy distribution over frequencies, $E(\omega) \sim \omega^{-3/2}$.

However, exploring the energy frequency spectrum in experiments with capillary waves is a rather difficult task. From the standpoint of an experimentalist, it is most convenient to explore not the energy distribution E_ω but the pair correlation function $I(\tau) = \langle \eta(r, t+\tau)\, \eta(r, t) \rangle$ for the deviation of the surface elevation from equilibrium at a point r, because the deviation $\eta(r, t)$ from a planar surface is directly measurable.

The wave turbulence theory [4] for a system of capillary waves on the surface of a liquid predicts the formation of a turbulent cascade in the inertial range bounded by the pumping at low frequencies and the dissipation range at high frequencies. Within the inertial range, the pair correlation function $I(\tau)$ in the Fourier representation is described by a power-law function of the frequency (turbulent cascade):

$$I_\omega \sim \omega^{-m} , \qquad (3)$$

and $E(\omega) \sim \omega^{4/3} I_\omega$. The exponent m depends on the spectral characteristics of the driving force. Under the excitation of the surface of the liquid by a low-frequency noise in a broad band $\Delta\omega$ (with a bandwidth exceeding the characteristic pumping frequency ω_p, $\Delta\omega \geqslant \omega_p$), the turbulent cascade I_ω is described by the function ω^{-m} with the exponent $m = 17/6$. Numerical simulations [5] provide an estimate of m that is close to the theoretical prediction. The results of numerical modeling in Ref. [6] indicate that as the bandwidth of noise pumping $\Delta\omega$ is reduced, a series of equidistant peaks emerges in the turbulent cascade, with their widths behaving as a linear function of the frequency. For a narrow-band pumping, $\Delta\omega < \omega_p$, the decrease in the height of these peaks as the frequency increases is described by a power-law function of frequency with an exponent that exceeds the value for broadband noise pumping by one, i.e., $m = 23/6$.

Our experimental studies on the surface of liquid hydrogen have shown that the spectral characteristic of the applied force determines the value of the power-law exponent [7]. When the surface is perturbed by a low-frequency harmonic force, the correlation function I_ω exhibits a set of narrow peaks whose frequencies are multiples of the pumping frequency ω_p. The peak maxima are well described by a power law ω^{-m} with $m = 3.7 \pm 0.3$. When, in addition to pumping at a single resonance frequency, a harmonic force at another resonance frequency is applied, the exponent decreases to $m = 2.8 \pm 0.2$. The exponent was also close to $m = 3 \pm 0.3$ when the surface was excited by a broadband low-frequency noise. In these experiments, we have qualitatively shown that in passing from the surface excitation with broadband noise to pumping by a harmonic force at the single-cell resonance frequency, the exponent m increases. Detailed results characterizing the evolution of a turbulent

L V Abdurakhimov, M Yu Brazhnikov, A A Levchenko, I A Remizov, S V Filatov Institute of Solid State Physics, Russian Academy of Sciences, Chernogolovka, Moscow region, Russian Federation
E-mail: levch@issp.ac.ru

Uspekhi Fizicheskikh Nauk **182** (8) 879 – 887 (2012)
DOI: 10.3367/UFNr.0182.201208i.0879
Translated by S D Danilov; edited by A M Semikhatov